NOISE-INDUCED PHASE SYNCHRONIZATION AMONG ANALOG OSCILLATOR CIRCUITS: EXPERIMENTAL RESULTS WITH DISCRETE MOS DEVICES

Akira Utagawa, Tetsuya Asai, Yoshihito Amemiya

Graduate School of Information Science and Technology,
Hokkaido University,
Kita 14, Nishi 9, Kita-ku, Sapporo, 060-0814 Japan,
Phone:+81-11-706-7147, Fax:+81-11-706-7890,
e-mail: utagawa@lalsie.ist.hokudai.ac.jp
WWW: http://lalsie.ist.hokdai.ac.jp/

Abstract—

Noise-induced synchronization occurs where individual neural oscillators are synchronized with each other when they accept common pulse perturbations randomly distributed in time [1]. In this paper, we demonstrate noise-induced synchronization among identical electrical oscillator circuits in experiments. We also show that nonidentical oscillators have the same peak frequency in a power spectrum when they receive a common perturbation.

I. Introduction

Arai *et al*. theoretically proved that individual nonlinear oscillators can be synchronized by applying common random impulses to the oscillators [1]. This finding implies that when one considers embedding multiple oscillators on LSIs, the phases of the oscillators are synchronized by the impulses and the noisy oscillators distributed on LSIs can be utilized for ubiquitous clock generators. We previously showed that such synchronization was achieved in electrical circuits using circuit simulations [2]. In this report, we show practical experiment results of phase synchronization among nonlinear oscillator circuits and our evaluation of device mismatches in the oscillators on phase synchronization.

II. Model & numerical simulations

In Arai *et al*.'s model [1], a FitzHugh-Nagumo oscillator was used to demonstrate noise-induced synchronization. In this study, we used the Wilson-Cowan oscillators that are suitable for analog CMOS implementation [3]. Its dynamics are given by

$$\dot{u}_i = -u_i + f_\beta(u_i - v_i) + I(t), \quad (1)$$
$$\dot{v}_i = -v_i + f_\beta(u_i - \theta), \quad (2)$$

where u_i and v_i represent the system variables of the i-th oscillator, θ the threshold, $I(t)$ the common random impulses, and $f_\beta(\cdot)$ the sigmoid function with slope β.

Figures 1 and 2 show the numerical simulation results of a single Wilson-Cowan oscillator receiving the random impulses given by

$$I(t) = \alpha \left\{ \sum_j \delta\left(t - t_j^{(1)}\right) - \delta\left(t - t_j^{(2)}\right) \right\}, \quad (3)$$

where $\delta(t) = \Theta(t) - \Theta(t-w)$ (Θ, w and t_j represent the step function, the pulse width and the positive random number with $t_j^{(1)} \neq t_j^{(2)}$ for all js, respectively). The system parameters were $\theta = 0.5, \beta = 10$, $\alpha = 0.5$, $w = 0.1$, and the averaged inter-spike interval of $|I(t)|$ was set at 100. We confirmed that the trajectory clearly fluctuated in the presence of noise $I(t)$ (Fig. 1), and we observed the limit-cycle oscillations (Fig. 2).

We conducted numerical simulations using ten Wilson-Cowan oscillators ($N = 10$, N : the number of oscillators). All the oscillators have the same parameters and accept (or do not accept) the common random impulses $I(t)$. The initial condition of each oscillator was randomly chosen. Figure 3 shows the raster plots of ten oscillators (vertical bars were plotted at which $u_i > 0.5$ and $du_i/dt > 0$). When the oscillators did not accept $I(t)$ ($\alpha = 0$), they exhibited independent oscillations as shown in Fig. 3(a). However, all the oscillators were synchronized when $\alpha = 0.5$ as shown in Fig. 3(b). To evaluate the degree of the synchronization, we used the following order parameter [4]:

$$R(t) = \frac{1}{N}\left|\sum_j \exp(i\phi_j)\right|,$$

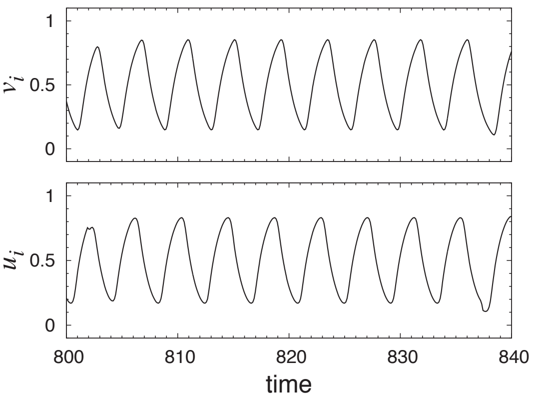

Fig. 1. Time courses of system variables of single Wilson-Cowan oscillator receiving common random impulses.

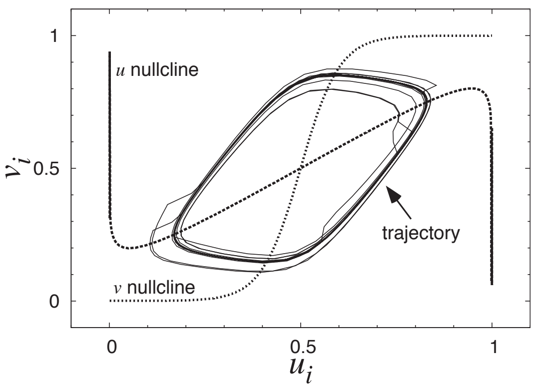

Fig. 2. Nullclines and trajectories of single Wilson-Cowan oscillator receiving common random impulses.

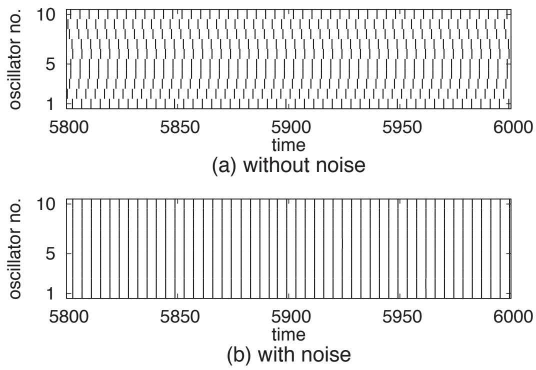

Fig. 3. Raster plots of ten oscillators: (a) independent oscillations without common random impulses and (b) synchronous oscillations with common random impulses.

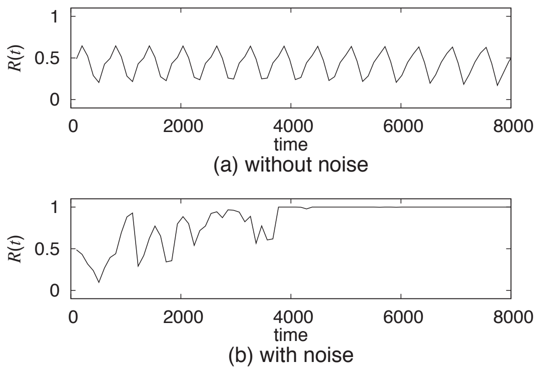

Fig. 4. Time courses of order parameter values: (a) without common random impulses and (b) with common random impulses.

where i the imaginary unit. When all the oscillators are synchronized, $R(t)$ equals 1 because of the uniform ϕ_js, while $R(t)$ is less than 1 if the oscillators are not synchronized. Figure 4 shows the time courses of the order parameter. When $\alpha = 0$, $R(t)$ was unstable and was always less than 1 [Fig. 4(a)], whereas $R(t)$ remained at 1 after it became stable at $t \approx 5000$ when $\alpha = 0.5$ [Fig. 4(b)]. These results indicate that if we implemented these oscillators as clock generators on CMOS LSIs, applying common random impulses to the oscillators could synchronize them.

III. Circuit structure

Figure 5 shows a schematic of the Wilson-Cowan oscillator circuit. Our oscillator circuit consists of a differential amplifier and a buffer circuit. In our experiments, a M-sequence generator was used as the noise source. C_1 and C_2 represent the capacitances, $V_{\rm bias}$ the bias voltage that determines the intrinsic frequency of the oscillator, r_0 the input resistance, and $V_{\rm dd}$ the supply voltage. The u_i and v_i in the figure obey the following equation,

$$\begin{aligned} C_1\dot{u_i} &= f'_{\beta_u}(u_i - v_i), &(4)\\ C_2\dot{v_i} &= f'_{\beta_v}(u_i - V_{\rm dd}/2), &(5)\end{aligned}$$

where $f'_\beta(\cdot) \approx \alpha(f_\beta(\cdot) - 0.5)$ (α and β are the device parameters), β_u is the device parameter determined by $V_{\rm bias}$ and $V_{\rm mseq}$, and β_v is the device parameter. The circuit's operation can be distinguished into four regions as follows:

i) $u_i > v_i$ & $u_i > V_{\rm dd}/2 : \dot{u_i} > 0$ & $\dot{v_i} > 0$,
ii) $u_i < v_i$ & $u_i > V_{\rm dd}/2 : \dot{u_i} < 0$ & $\dot{v_i} > 0$,
iii) $u_i < v_i$ & $u_i < V_{\rm dd}/2 : \dot{u_i} < 0$ & $\dot{v_i} < 0$,
vi) $u_i > v_i$ & $u_i < V_{\rm dd}/2 : \dot{u_i} > 0$ & $\dot{v_i} < 0$.

All the oscillators receive common random impulses ($V_{\rm mseq}$) produced by the same random sequence via capacitance C_0, which determines the strength of the noises. In the Wilson-Cowan system, the noise term $I(t)$ was added to u_i's dynamics only. In our circuit,

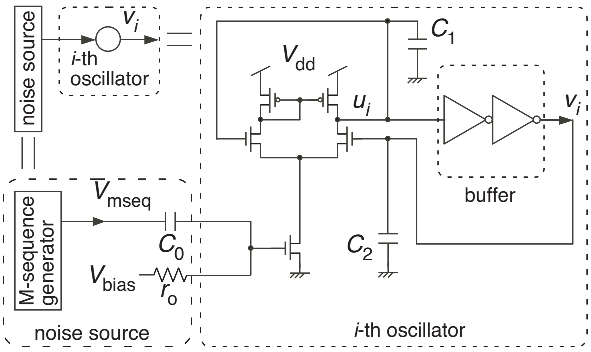

Fig. 5. Circuit construction of noisy oscillator

the noisy term was included in the slope factor β_u of OTA's $f'_{\beta_u}(u_i - v_i)$. The slope factor increases vastly as V_{bias} increases. Therefore, by fluctuating V_{bias} with V_{mseq} via C_0, one can perturb the circuit effectively.

IV. Measurement results

In the following experiments, we employed discrete devices (C_0 = 21 pF, C_1 = 4.7 nF, C_2 = 10.3 nF, r_0 = 1 kΩ, V_{dd} = 5 V, and V_{bias} = 1.5 V). The 4-bit M-sequence circuit was constructed using D-FF IC (HD14174BP) and Ex-OR IC (TC4030BP), and was operated at 20 kHz frequency. We used nMOSFET (2SK1398) and pMOSFET (2SJ184) for the differential amplifier, and used inverter ICs (TC4069BP) for the buffer circuit. In our experiments, we constructed a single oscillator, and measured it several times (total trial run: N) instead of constructing multiple oscillators and measuring them simultaneously. This is because device mismatches among the oscillators would strongly affect the experimental results, and here we wanted to control these effects.

We first observed the single oscillator's properties (N = 1). Figure 6(a) shows the time courses of u_i and v_i of the oscillator. We observed fluctuations in u_i and v_i due to common random impulses produced by the M-sequence generator. Figure 6(b) shows the trajectories of u_i and v_i of the measured oscillator. We confirmed limit-cycle oscillations and confirmed that their trajectories were clearly fluctuated around the limit-cycle orbit. Next we observed population activities of multiple oscillators ($N = 10$: 10 trials with the single oscillator). We applied the same initial conditions for each trial when no random impulses were applied, while we applied different initial conditions when common random impulses were applied. Figures 7(a) and (b) show raster plots where vertical bar were plotted at $v_i > V_{\text{dd}}/2$ and $dv_i/dt > 0$. When no random impulses were applied to the oscillators, their

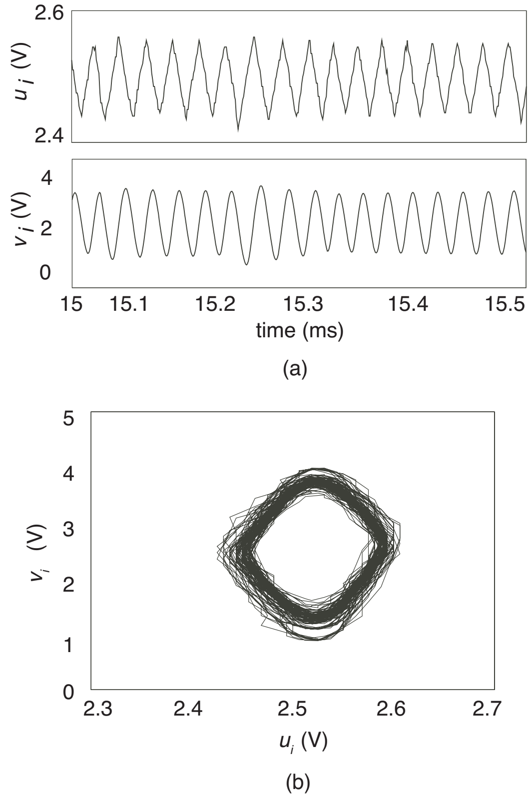

Fig. 6. Experimental results of single oscillator circuit: (a) time courses of u_i and v_i and (b) trajectories of u_i and v_i of noisy oscillator.

phases were desynchronized because no interaction occurred among the oscillators [Fig. 7(a)]. However, when random impulses were applied to all the oscillators, they exhibited phase synchronization although they didn't have any interaction [Fig. 7(b)] as predicted in Sect. 2. When all the oscillators are identical and environmental noise is small enough, the phase differences among the oscillators that receive common random impulses approach 0 as proved by Arai *et al*. [1]. Figure 7 (c) shows the time course of the $R(t)$ without random impulses (dotted line) and with random impulses (solid line). $R(t)$ was almost 1 when $t = 0$, but $R(t)$ immediately deceased as t increased and stayed at a low value when random impulses were not given. This means that time-dependent small (but unavoidable) environmental noises led to the desynchronization. When random impulses were applied, phases of the oscillators were almost random at $t = 0$, so $R(t)$ was around 0. Then $R(t)$ gradually approached to 1 at 25–30 ms. This demonstrated that phase synchronization among the individual oscillators was stochastically induced by random impulses.

Finally, we examined the effects of device mis-

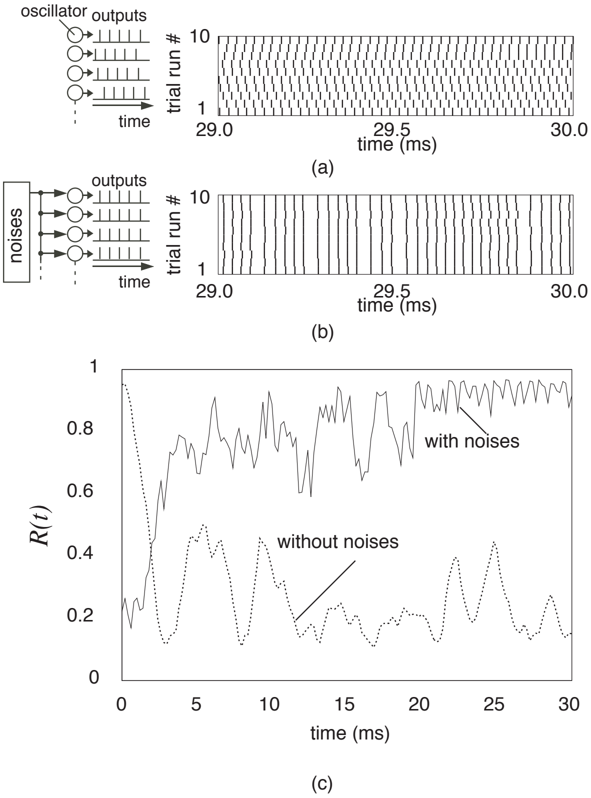

Fig. 7. Experimental results: (a) raster plots of 10 oscillators without random impulses, (b) raster plots of 10 oscillators with random impulses, and (c) time course of order parameters

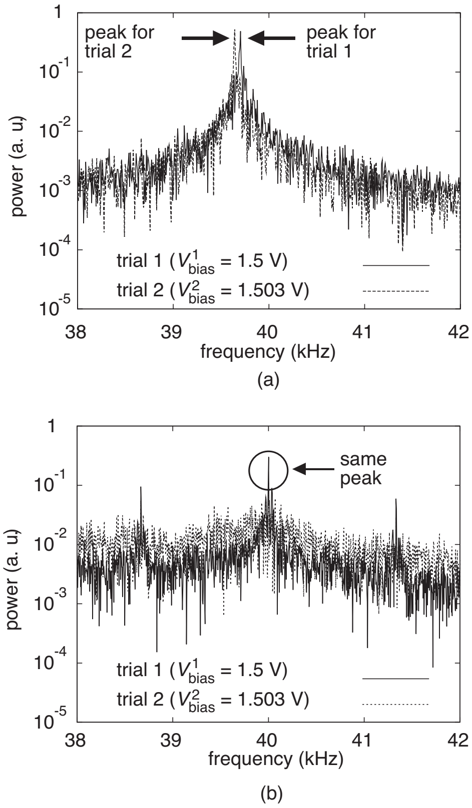

Fig. 8. Power spectrum for oscillators: (a) without random impulses and (b) with random impulses

matches on the phase synchronization. Although the results shown in Fig. 7 demonstrated that the oscillators were synchronized by random impulses, the variation in circuit characteristics would not be negligible in practical situations. We mimicked these effects in the way described in our previous work [2]; *i.e.*, $V_{\rm bias}$ which determines the oscillators' intrinsic frequency was distributed as the most significant parameter. We compared the results between two trials ($N = 2$). In the first trial, we measured a circuit with bias condition $V^1_{\rm bias}$ = 1.5 V. At the second trial, we measured the circuit with $V^2_{\rm bias} = V^1_{\rm bias}$ - 3 mV. Figure 8 shows the power spectrums of the oscillator outputs (v_i). When no random impulses were applied [Fig. 8(a)], the oscillators had a different peak frequency because their intrinsic frequencies were governed by $V^1_{\rm bias}$ and $V^2_{\rm bias}$. However, when random impulses were applied [Fig. 8(b)], the oscillators in both trials had the same peak frequency, although their intrinsic frequencies were different. This indicates that even if small transistor mismatch occurs in the oscillators, their phases would be synchronized.

V. Conclusion

We experimentally tested noise-induced synchronization among electrical oscillator circuits receiving common random impulses. The oscillators exhibited phase synchronization when they received random impulses, whereas they exhibited desynchronization when they didn't received random impulses. When small transistor mismatch occurs in oscillators, the oscillators still have the same peak frequency in the power spectrum when receiving random impulses.

References

[1] K. Arai and H. Nakao, "Phase coherence in an ensemble of uncoupled limit-cycle oscillators receiving common Poisson impulses," in *Phys. Rev. E*, **77**, p.p. 036218, 2007.

[2] A. Utagawa, T. Asai, T. Hirose, and Y. Amemiya, "Noise-induced synchronization among sub-RF CMOS analog oscillators for skew-free clock distribution," in *IEICE Trans. on Fundamentals*, **E91-A**, p.p 2475–2481, 2008.

[3] T. Asai, Y. Kanazawa, T. Hirose, and Y. Amemiya. Analog reaction-diffusion chip imitating the Belousov-Zhabotinsky reaction with Hardware Oregonator Model, in *Int. J. of Unconventional Computing*, vol. 1, no. 2, p.p. 123–147, 2005.

[4] Y. Kuramoto, *Chemical Oscil lation, Waves, and Turbulence,* Springer-Verlag, Tokyo, 1984; Dover Edition, 2003.